1992

Performance Improvement of a Vaneless Diffuser of Centrifugal Compressor

Y. Adachi
Daikin Industries

A. Otsuki
Daikin Industries

K. Bantle
Osaka University; Japan

Y. Miyake
Osaka University; Japan

PERFORMANCE IMPROVEMENT OF A VANELESS DIFFUSER OF CENTRIFUGAL COMPRESSOR

Yasunori ADACHI, Daikin Industries,Ltd. 1-1 Nishi Hitotsuya ,Settsu, Osaka 566, JAPAN
Kiyoshi BANDO, Osaka University, 2-1 Yamada-oka, Suita, Osaka 565, JAPAN
Yutaka MIYAKE, Osaka University
Akira OTSUKI, Daikin Industries,Ltd

ABSTRACT

Performance tests were conducted for centrifugal compressors having vaneless diffusers whose flow passages are tapered at diffuser outlet portion. Both the beginning point of the tapered passage and its tapered throttle ratio were optimized experimentally. The optimum value of the tapered throttle ratio was 0.5. Both the surge margin and the compressor efficiency were improved over a wide range of flow rates, as compared with a compressor with a parallel wall diffuser. At surge inception, the static pressure difference between the two walls of the diffuser inlet decreased as the tapered passage width reduced at the diffuser outlet. The static pressure difference at surge inception was peculiar to a compressor independent of the conditions of inlet guide vane opening. Therefore, surge inception can be predicted by detecting the pressure difference at the diffuser inlet.

NOMENCLATURE

$C_{R,b-d}$	:	Static pressure recovery ratio $= (p_d - p_b)/(p'_b - p_b)$
$C_{R,b-e}$	:	Static pressure recovery ratio $= (p_e - p_b)/(p'_b - p_b)$
g	:	Acceleration of gravity
H	:	Adiabatic head
IVO	:	Inlet guide vane opening
p	:	Static pressure
p'	:	Total pressure
Q	:	Suction flow rate
R_1	:	Radius of impeller outlet
R_2	:	Radius of diffuser inlet
R_3	:	Radius where tapered passage begins
R_4	:	Radius of diffuser outlet
t_1	:	Impeller outlet width
t_2	:	Diffuser inlet width
t_4	:	Minimum width of tapered passage at diffuser outlet
U_1	:	Impeller circumferential velocity
Δp	:	Static pressure difference between the hub and shroud walls of diffuser inlet $= p_a - p_b$
ε	:	Tapered throttle ratio $= t_4/t_2$ (ratio of parallel passage width and minimum width of tapered passage)
ϕ	:	Flow coefficient $= Q/(\pi R_1^2 U_1)$
ψ	:	Pressure coefficient $= gH/U_1^2$
$\delta\psi$	:	Pressure coefficient of surge margin $= 0.04$
η	:	Adiabatic efficiency of compressor on the performance evaluation line (e.g., broken line in Fig.5)

Subscripts

1	:	Impeller outlet
2	:	Diffuser inlet
3	:	Point where tapered passage begins
4	:	Diffuser outlet
a, b, c, d, e	:	Point where diffuser pressure was measured(Fig.3)
SL	:	Surge line

INTRODUCTION

Due to the recent trend toward energy saving, the requirement for high efficiency is growing. We ,therefore, investigated how we can increase efficiency of large size centrifugal chillers which are applied to the commercial and industrial air conditioning. To improve the performance of centrifugal compressors, it is essential to improve the characteristics of the impeller and the diffuser. The refrigerant flow at the impeller exit is three dimensionally distorted and temporally fluctuating. In addition, this flow is complicated and varies by the operating conditions. We, therefore, investigated the refrigerant flow in the diffuser and could reduce the loss by effectively recovering the static pressure and increase the surge margin.

It is well known that the refrigerant flow inside a compressor can be stabilized by adding resistance at the diffuser exit[1][2]. The reports on the rotating stall limit and the improvement of surge margin are those related to the vaned diffusers[3,4,5] and the vaneless diffusers[6,7]. Wire nettings or porous barriers[3], throttle[1,4,6], adjustable circular exit vanes[5,7] are used for putting up resistance. Some reports explain that the loss caused by the resistance increases as the flow rate increases and as a result the negative gradient range of the combined flow vs pressure characteristic curve is enlarged and the flow is stabilized[4,6]. Therefore, in the range of low flow rate, the loss caused by the resistance is small but in the range of high flow rate, the loss is large, and accordingly the performance drops remarkably[4,6].

This paper deals with the method of improving both surge margin and efficiency even at high flow rate by adding tapered passage at the vaneless diffuser outlet portion. The optimum results are obtained by determining the optimum combination of the beginning point of the tapered passage at the diffuser outlet and its tapered throttle ratio.

The flow distortion at the vaneless diffuser inlet is explained in many reports related to the velocity distortion[4,5,9,10]. On the other hand, according to our test results, the surge occurs when the static pressure difference between the hub and shroud walls of the diffuser inlet exceeds a critical condition which is peculiar to a compressor. In addition, this report also deals with the prediction of surge inception based on the test results.

TESTING DEVICE AND TESTED COMPRESSORS

Fig.1 shows the refrigeration system diagram ($1 \rightarrow 2 \rightarrow 3 \rightarrow 4 \rightarrow 1$) of the testing apparatus using CFC11. Fig.2 shows a cross section of the tested compressor. The compressor is driven by a motor and the impeller speed is increased to 9,200 r.p.m by the sun and star step-up gears. The impeller is double shroud type with blades having backswept angle of 60 degrees at the exit. Movable inlet guide vanes are located upstream of the impeller and the prerotation is zero at IVO of 80%. The tests were conducted for four kinds of vaneless diffusers as shown in Table 1.

Under a constant inlet guide vane opening, we varied the compressor head by varying the temperatures of a condenser and an evaporator and carried out the following measurements. We measured the adiabatic head and the adiabatic efficiency of the compressor from the total temperature and the total pressure in the suction and discharge pipes shown in Fig.1. We measured the suction flow rate by using an orifice flow meter installed at the suction pipe. As shown in Fig.3, we measured the static pressure in the diffuser at the points *a*, *b*, *c*, *d*, *e* and the total pressure at the points *b*, *d*, *e*. We repeated the above measurements for many kinds of inlet guide vane openings.

The measuring method of the static and total pressures is shown in Fig.4(a) and (b), respectively. The inner diameter of the static pressure probe shown in Fig.4(a) is 2 mm and that of the total pressure probe shown in Fig.4(b) is 1.5 mm. The total pressure probe is placed at the widthwise center of the diffuser. The pressures were measured by varying the probe angle and the pressure which showed the maximum value was regarded as the total pressure. The static and total pressure probes are connected to pressure transducers at points 300 mm away from the diffuser wall and the data were processed on computers.

TEST RESULTS AND DISCUSSION

Beginning Point of Tapered Passage

Fig.5 shows the characteristic curve of compressor C1. In this figure, ϕ denotes the flow coefficient measured in the compressor suction pipe and ψ denotes the pressure coefficient obtained from the total pressure and total temperature measured in the suction and discharge pipes. Symbols ○ show the measured data, solid lines show the characteristic curves at the constant IVO and the chain line shows the surge line. The broken line shows a performance evaluation line of the compressor. The performance evaluation line is obtained by subtracting $\delta\psi$ along the constant IVO line from the value of ψ on the surge line, where $\delta\psi$ is the pressure coefficient of surge margin taken as 0.04. Data near the surge line are the average values of fluctuated data. A surge inception point was defined as a point where the pressure difference reading of the orifice flow meter starts fluctuating.

Point A in Fig.5 shows a design point of compressor C1 and Fig.6 shows the test result of pressure distribution in the compressor C1 at this point. This figure shows that the static pressure recovery in the diffuser is approximately 90% completed at the point d. As shown in Fig.3, therefore, we determined that a tapered flow passage inclined about 20 degrees from the radial direction (hereinafter referred to as tapered passage or tapered throttle) should begin from the point of radius 345 mm ,that is located around the midpoint between the points d and e.

Surge Margin and Tapered Throttle at Diffuser Outlet

In order to investigate the influence of tapered throttle at diffuser outlet, performance tests were conducted for compressors C2, C3 and C4 of which tapered throttle ratios $\varepsilon(=t_4/t_2)$ are 0.75, 0.5 and 0.25, respectively. Figs.7, 8 and 9 show characteristic curves of compressors C2, C3 and C4, respectively. Fig.10 shows the surge lines and IVO 100% lines of compressors C1, C2, C3 and C4. This figure shows that as the tapered throttle ratio ε becomes smaller ,namely , the tapered flow passage width at the diffuser outlet becomes smaller, surge margin is more enlarged. However, if the tapered throttle ratio extremely decreases as is the case of compressor C4, the maximum flow rate decreases largely.

Fig.11 shows the pressure coefficient on the surge lines of compressors C1, C2 and C3. The pressure coefficient of compressors C2 and C3 is divided by that of the compressor C1. As the flow rate decreases, the pressure coefficients of compressors C2 and C3 increase from that of compressor C1. As a result, surge margin of compressors C2 and C3 is improved.

According to the investigation on vaneless parallel-wall diffuser by Kobayashi et al.[11], the diffuser inlet shape does not affect the surge margin.

Though it is not mentioned in this report, we conducted a performance test for the same compressor as this report by varying the diffuser inlet width ratio (t_2/t_1) from 0.6 to 1.0 without the tapered throttle at the diffuser outlet. The test results show no improvement of surge margin. On the contrary, test results with tapered throttle at the diffuser outlet show the improvement of surge margin as mentioned above.

Efficiency and Tapered Throttle at Diffuser Outlet

Fig.12 shows the adiabatic efficiency ratio (adiabatic efficiency of compressors C1, C2, C3, C4 divided by a maximum efficiency $\eta_{C3,max}$ of compressor C3). Efficiency at a performance evaluation point of each compressor is defined as the adiabatic efficiency. The broken line in Fig.5 shows the performance evaluation line for compressor C1 as an example.

The efficiency of the compressor C3 is improved over a wide range of flow rate except for maximum flow rate range as compared with that of compressor C1. The efficiency of compressor C4 is decreased remarkably except for the low flow rate range.

Fig.13 shows the correlation between the tapered throttle ratio ε and the maximum value of each efficiency curve shown in Fig.12. From Figs.12 and 13 we found that the optimum tapered throttle ratio ϵ is 0.5.

Fig.14 shows the static pressure recovery ratio $C_{R,b-d}$ of compressors C1, C3 from the point b to d in Fig.3. Fig.15 shows the static pressure recovery ratio $C_{R,b-e}$ from the point b to e. These

static pressure recovery ratios are shown as a function of pressure coefficient ψ at 80% IVO for each compressor. The chain lines in these figures show the surge inception lines. The pressure recovery ratio of compressor C3 is improved by approximately 10 to 20% compared with that of compressor C1.

Prediction of Surge Inception Point

The static pressure differences Δp between the hub (point a in Fig.3) and shroud (point b in Fig.3) walls of the diffuser inlet were measured. Figs.16, 17 and 18 show the correlation between the pressure difference Δp and the pressure coefficient ψ under the constant IVO for compressors C1, C2 and C3, respectively. In these figures, shaded area shows the surge region.

The static pressure on the shroud wall at the diffuser inlet tends to become lower than the pressure on the hub wall as the pressure coefficient ψ increases, or the flow rate coefficient ϕ decreases. Furthermore, the static pressure difference Δp_{SL} at surge inception has a peculiar constant value independent of inlet guide vane openings. The Δp_{SL} values are peculiar to each compressor and for compressors C1, C2 and C3, they are 0.38, 0.30 and 0.28 kg/cm^2, respectively. As the tapered flow passage width at diffuser outlet decreases, the static pressure difference Δp_{SL} decreases.

The blade exit angle of the tested impeller is 60 degrees. Due to this large angle, the surge is likely to occur at the diffuser. Figs.16, 17 and 18 show that the static pressure difference at the diffuser inlet bears strong correlation with the surge inception. In addition, the static pressure difference at surge inception bears no relation to the inlet guide vane openings. Therefore, surge inception can be predicted by detecting the static pressure difference between the hub and shroud walls at the diffuser inlet.

However, the process of flow behavior to surge inception point is different by each compressor. The compressor C1 generated an abnormal sound which is presumed to be a symptom of the rotating stall but compressors C2 and C3 having the tapered throttle at the diffuser outlet showed sudden inception of the surge without the distinct symptom of the rotating stall.

We consider the dimensionless evaluation of the pressure differences Δp_{SL} as a subject to be investigated in the future.

Fig.19 shows the relation of the static difference at the diffuser inlet and the pressure coefficient at 100% IVO for compressors C1 and C3. By adding the tapered throttle at the diffuser outlet, the static pressure difference decreases over a whole range of pressure coefficient. This decrease of the static pressure difference at the diffuser inlet contributes to the decrease of the flow distortion. As a result, the surge margin, the adiabatic efficiency and the static recovery ratio are improved as shown in Figs.10, 11, in Figs.12, 13 and in Figs.14, 15.

Application to Actual Compressors

In general, the diffuser outlet of a centrifugal compressor has spreading out shape and is smoothly connected to the scroll. On the other hand, it is reported that surge margin can be improved by adding resistance such as retractable diffuser exit rings[4], adjustable exit vanes[5] and throttling valves[6]. However, to the best of authors' knowledge, no such resistances are put into practical use in refrigeration field. It is probably because the performance drops in the region of high flow rate[4,6] by adding these resistances.

Our test results show that the efficiency improvement in the high flow rate can be achieved by determining the optimum combination of the beginning point of the tapered passage and the tapered throttle ratio at the diffuser outlet. It might be possible to improve performance by using complicated mechanism such as adjustable exit vanes[5] but it is easier to put the method as explained in this paper into practical use.

CONCLUSIONS

Performance tests were conducted for centrifugal compressors having vaneless diffusers of which tapered throttle ratios ε at the diffuser outlet are 1.0, 0.75, 0.5, 0.25 and the test results are summarized as follows.

(1) It is desirable to determine the beginning point of the tapered passage at diffuser outlet around the point where static pressure recovery in the diffuser is almost completed.

(2) As the tapered throttle ratio ε becomes small or the tapered passage width at diffuser outlet becomes small, surge margin is improved. However, if the tapered throttle ratio is too small($\varepsilon \simeq 0.25$), the maximum flow rate decreased and the adiabatic compressor efficiency remarkably drops.

(3) The optimum tapered throttle ratio for the tested compressor is 0.5, and the compressor efficiency is improved over a wide range of flow rate, as compared with a compressor with a parallel passage diffuser.

(4) The static pressure on the shroud wall at the diffuser inlet tends to become lower than the static pressure on the hub wall as the pressure coefficient ψ increases or the flow rate ϕ decreases.

(5) As the tapered throttle ratio at diffuser outlet decreases, the static pressure difference Δp_{SL} of the diffuser inlet at surge inception decreases.

(6) Irrespective of the inlet guide vane openings, when the static pressure difference at the diffuser inlet exceeds the value which is peculiar to the compressor, the surge occurs. However, the static pressure difference Δp_{SL} changes its value depending on the tapered throttle ratio ε.

(7) Surge inception can be predicted by detecting the pressure difference between the two walls of the diffuser inlet.

REFERENCES

[1]Eckardt, D. , " Instantaneous Measurements in the Jet - Wake Discharge Flow of a Centrifugal Compressor Impeller " , ASME Journal of Engineering for Power, Vol. 97 , No. 3 , 1975 , pp. 337 - 346.

[2]Greitzer , E. M. , " The Stability of Pumping Systems - The 1980 Freeman Scholar Lecture " , ASME Journal of Fluids Engineering , Vol. 103 , No. 2 , 1981 , pp. 193 - 242.

[3]Imaichi, K. and Tsurusaki, H ., "Rotating Stall in a Vaneless Diffuser of a Centrifugal Fan " , Flows in Primary and Non - Rotating Turbomachinery Passages , ASME Winter Annual Meeting , 1979 , pp. 23 - 31.

[4]Abdelhamid , A. N. , " Control of Self - Excited Flow Oscillations in Vaneless Diffuser of Centrifugal Compression Systems " , ASME Paper , 82 - GT - 188 , 1982.

[5]Abdel - Hamid , A. N. , " A New Technique for Stabilizing the Flow and Improving the Performance of Vaneless Radial Diffusers " , ASME Journal of Turbomachinery , Vol. 109 , No. 1 , 1987 , pp. 36 - 40.

[6]Dussourd , J. L. , Pfannebecker , G. W. and Singhania , S. K. , " An Experimental Investigation of the Control of Surge in Radial Compressors Using Close Coupled Resistances " , ASME Journal of Fluids Engineering , Vol. 99 , No. 1 , 1977 , pp. 64 - 75.

[7]Railly, J . W. and Ekerol, H . "Influence of a Closely Coupled Throttle on the Stalling Behavior of a Radial Compressor Stage" , ASME Journal of Engineering for Gas Turbine and Power , Vol. 107 , No. 2 , 1985 , pp. 522 - 527.

[8]Fuzii , S. , " On Stability and Surging of Centrifugal Pump (in Japanese) " , Transactions of JSME , Vol. 13 , No. 44 , 1947 , pp. 184 - 191.

[9]Senoo, Y. , Kinoshita, Y. and Ishida, M. , " Asymmetric Flow in Vaneless Diffusers of Centrifugal Blowers " , ASME Journal of Fluids Engineering, Vol. 99 , No. 1 , 1977 , pp. 104 - 114.

[10]Yoshinaga , Y. , Kobayashi , H. and Kaneki , T. , " A Study on Performance of a Diffuser of Centrifugal Compressor , (in Japanese) " , Transactions of JSME (B) , Vol. 50 , No. 460 , 1984 , pp. 2943 - 2952.

[11]Kobayashi , H. , Nishida , H., Takagi , T. and Fukushima , Y. , " A Study on the Rotating Stall of Centrifugal Compressors (2nd Report , Effect of Vaneless Diffuser Inlet Shape on Rotating Stall) , (in Japanese) " , Transactions of JSME (B) , Vol. 56 , No. 529 , 1990 , pp. 2646 - 2651.

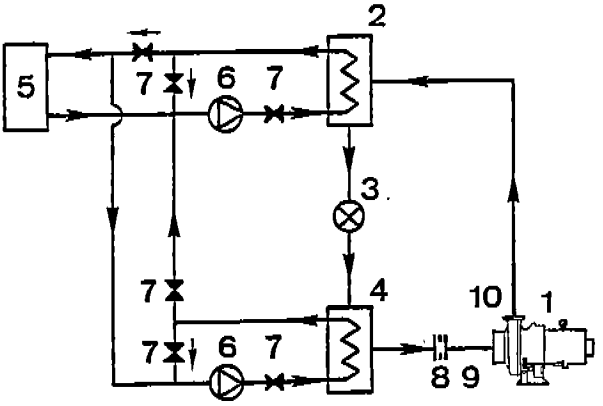

1	:	Compressor	6	:	Pump
2	:	Condenser	7	:	Control valve
3	:	Float valve	8	:	Orifice flow meter
4	:	Evaporator	9	:	Suction pipe
5	:	Cooling tower	10	:	Discharge pipe

Fig.1 Refrigeration system of experimental apparatus

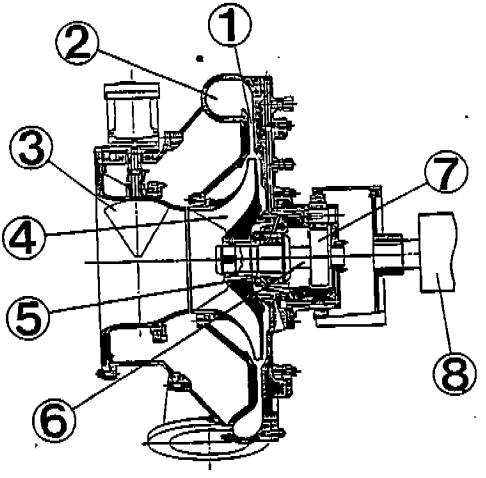

1	:	Diffuser	5	:	Insert bearing
2	:	Scroll	6	:	Rotation shaft
3	:	Inlet guide vane	7	:	Sun and star gears
4	:	Impeller	8	:	Motor

Fig.2 Cross section of tested compressor

Table 1 Specifications of four kinds of tested vaneless diffusers

Compressor	C1	C2	C3	C4
R_1	220			
R_2	240			
R_3	345			
R_4	375			
t_1	18.3			
t_2	15.0			
t_4	15.0	11.2	7.5	3.8
R_2/R_1	1.09			
R_3/t_2	23.0			
R_4/t_2	25.0			
t_2/t_1	0.82			
$\epsilon = t_4/t_2$	1.0	0.75	0.5	0.25

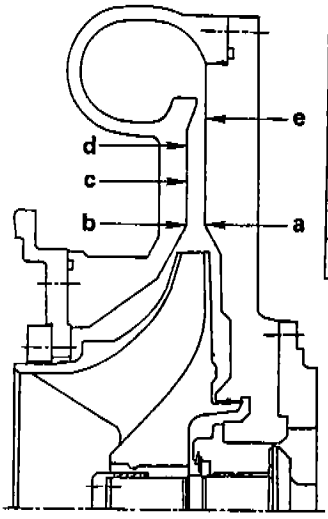

Radii of pressure measuring points	
a	241 mm
b	241 mm
c	290 mm
d	330 mm
e	355 mm

Fig.3 Measuring points of pressure in the diffuser

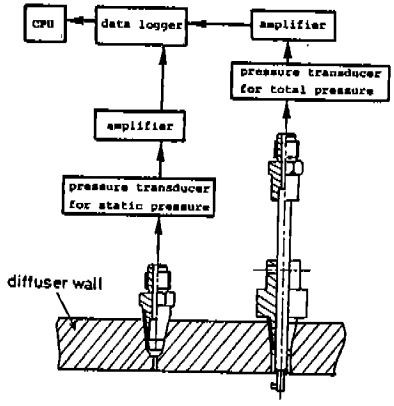

(a)Static pressure (b)Total pressure

Fig.4 Measuring method of pressure

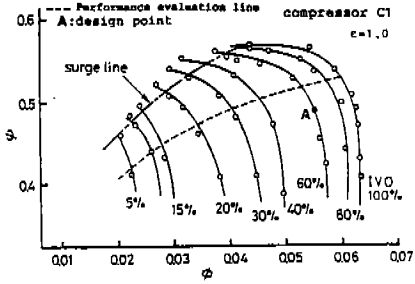

Fig.5 Characteristic curve of compressor C1

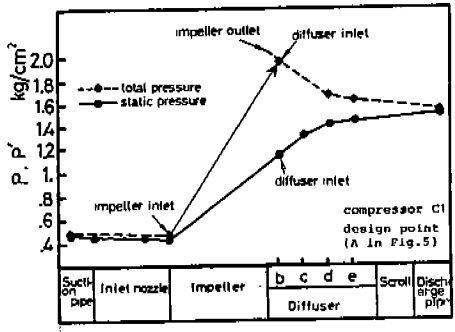

Fig.6 Pressure distribution at design point of compressor C1

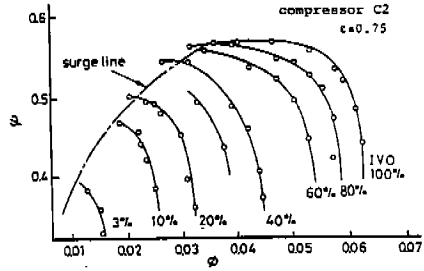

Fig.7 Characteristic curve of compressor C2

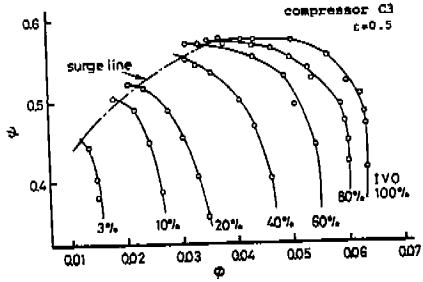

Fig.8 Characteristic curve of compressor C3

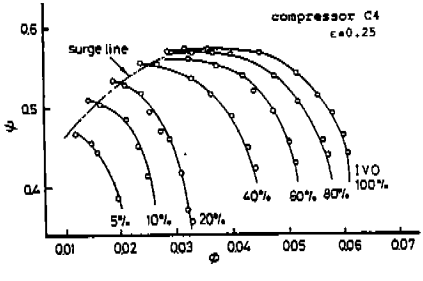

Fig.9 Characteristic curve of compressor C4

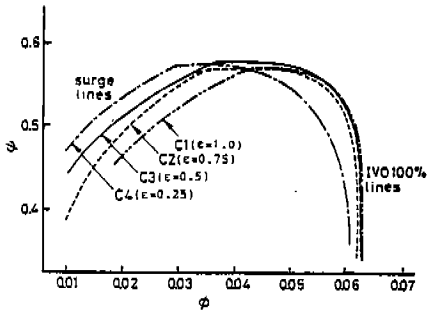

Fig.10 Surge lines and IVO 100% lines of compressors C1, C2, C3 and C4

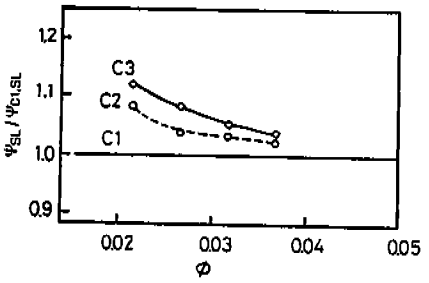

Fig.11 Pressure coefficient on the surge lines of compressors C1, C2 and C3

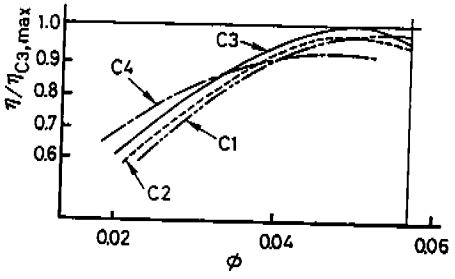

Fig.12 Adiabatic efficiency ratio of compressors C1, C2, C3 and C4 (value on performance evaluation lines for $\delta\psi = 0.04$)

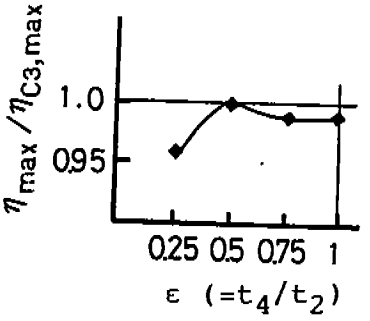

Fig.13 Correlation between the tapered throttle ratio ε and the maximum value of each adiabatic efficiency curve shown in Fig.12

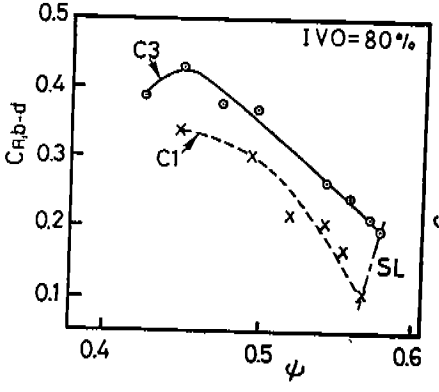

Fig.14 Static pressure recovery ratio of compressors C1 and C3 from the point b to d of diffuser (IVO=80%)

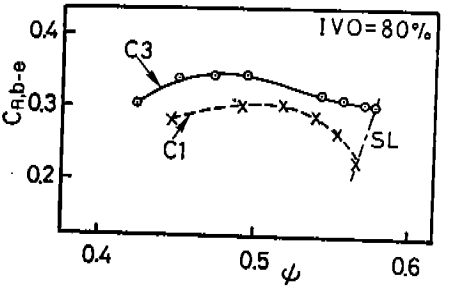

Fig.15 Static pressure recovery ratio of compressors C1 and C3 from the point b to e of diffuser (IVO=80%)

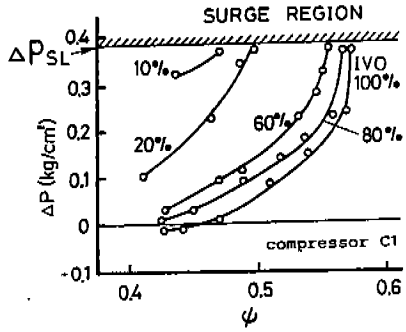

Fig.16 Correlation between the static pressure difference Δp and the pressure coefficient ψ under constant IVO for compressor C1

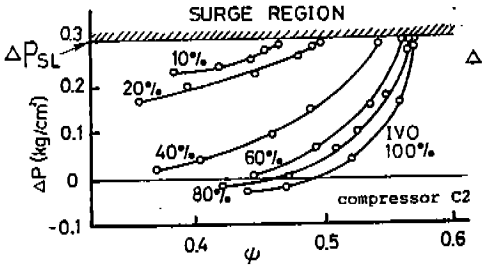

Fig.17 Correlation between the static pressure difference Δp and the pressure coefficient ψ under constant IVO for compressor C2

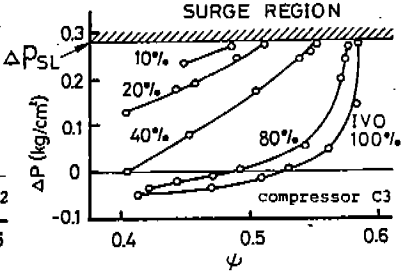

Fig.18 Correlation between the static pressure difference Δp and the pressure coefficient ψ under constant IVO for compressor C3

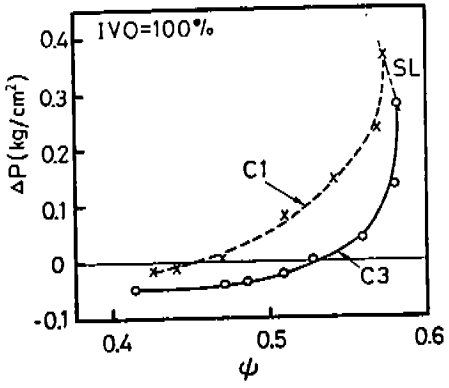

Fig.19 Relation between the static pressure difference at diffuser inlet and the pressure coefficient at IVO 100% for compressors C1 and C3